Supporting Information

Scalable Large-Area p–i–n Light-Emitting Diodes Based on WS_2 Monolayers Grown via MOCVD

Dominik Andrzejewski[1], Henrik Myja[1], Michael Heuken[2,3], Annika Grundmann[3], Holger Kalisch[3], Andrei Vescan[3], Tilmar Kümmell[1,], Gerd Bacher[1]*

[1] Werkstoffe der Elektrotechnik and CENIDE, Universität Duisburg-Essen, 47057 Duisburg, Germany

[2] AIXTRON SE, 52134 Herzogenrath, Germany

[3] Compound Semiconductor Technology, RWTH Aachen University, 52074 Aachen, Germany

KEYWORDS

tungsten disulfide monolayer, metal organic chemical vapor deposition, light emitting device, 2D LED, 2D semiconductor, electroluminescence, luminance

Temperature-dependent photoluminescence experiments

To get a deeper insight into the luminescence behavior of the grown WS_2 monolayer on sapphire, temperature-dependent PL measurements were made. Selected PL spectra at different temperatures between 5.6 K to 300 K are shown in Figure S1(a). While at room temperature only exciton emission at the bandgap is observed, defect-related emission becomes more and more prominent at low temperatures. The inset of Figure S1(a) shows PL spectra at 150 K and 300 K, recorded with an enhanced spectral range, clearly indicating bandgap as well as defect-related emission below the bandgap at reduced temperatures. The latter might be attributed e.g., to sulfur vacancies.[1] As the integrated PL intensity increases by a factor of about 400 when reducing the temperature from 300 K to 5.6 K, non-radiative recombination via defects (e.g. via Shockley–Read–Hall processes) apparently limits the PLQY at room temperature. Over this temperature range a shift of the PL peak of about 80 meV is observed, in agreement with literature for exfoliated WS_2 monolayer.[2] The shift of the peak position is plotted in Figure S1(b) as function of temperature and is fitted with eq S1 of O'Donnell *et al.*:[3]

$$E(T) = E_0 - 2S\frac{\langle\hbar\omega\rangle}{\exp\left(\frac{\langle\hbar\omega\rangle}{k_B T}\right)-1} \qquad \text{(eq S1)}$$

where E_0 is the optical bandgap at zero temperature, S is a dimensionless coupling constant, k_B is the Boltzmann constant, and $\langle\hbar\omega\rangle$ is an average phonon energy. From the fitting, S is extracted to be 2.58 and $\langle\hbar\omega\rangle$ corresponds to 25.7 meV. These values have also been observed in the literature for exfoliated WS_2 monolayers, which confirms a good crystal growth with the used MOCVD process.[4]

The FWHM of the A exciton emission is depicted in Figure S1(c) as function of the temperature. The broadening from about 23.5 meV at 5.6 K to 42 meV at 300 K is confirm with the mean value of the PL map in Figure 2(c) of 12.6 nm, which is equivalent to 42.7 meV in this spectral range. The temperature-dependent linewidth (FWHM) of excitons due to interaction

with LO phonons in semiconductors in general as well as in TMDC monolayers can be expressed as[5,6]

$$FWHM(T) = \Gamma_0 + \frac{\Gamma_{LO}}{\exp\left(\frac{\Theta_{LO}}{T}\right)-1} \qquad \text{(eq S2)}$$

where Γ_0 represent the broadening from temperature independent mechanisms, Γ_{LO} the strength of the exciton–LO phonon coupling and Θ_{LO} the LO phonon temperature. Fitting the broadening with eq S2 a fixed phonon energy of 44.3 meV was assumed according to the LO phonon energy derived by Molas *et al.*[7] from Raman spectroscopy. The obtained LO phonon temperature Θ_{LO} of 514 K is in good agreement with literature.[8] Despite this the fitted curve provides a coupling strength Γ_{LO} of 80 meV. From these data we conclude that the FWHM at room temperature is controlled by exciton–LO phonon scattering rather than by inhomogeneous broadening effects. Note that at low temperatures (5.6 K) the MOCVD grown WS_2 monolayer exhibits approximately a doubled linewidth as compared to exfoliated WS_2 single crystals.[6,8] Furthermore, beside the excitonic PL an additional defect related emission at 1.94 eV is observed at low temperatures.

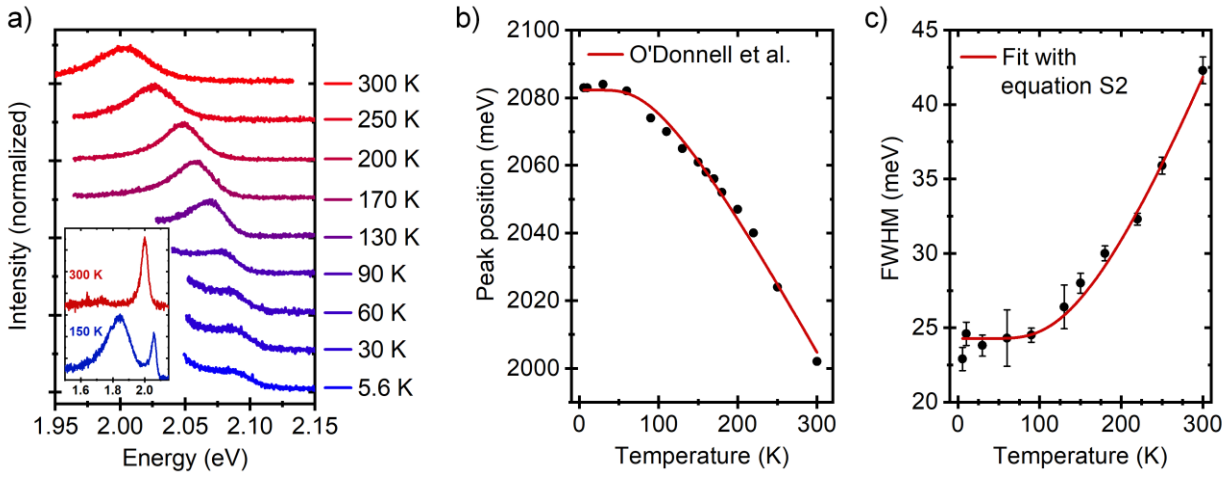

Figure S1. (a) Temperature-depended PL spectra of a WS_2 monolayer grown by MOCVD on sapphire. For excitation the 442 nm laser line of a He–Cd laser was used at a power density of 3 W/cm^2. The inset shows PL spectra at 150 K and 300 K, recorded with an enhanced spectral range, clearly indicating a pronounced contribution of defect related emission in the lower energy range at decreasing temperature. (b) Peak position of the measured PL spectra as function of temperature (black dots) compared to a fit curve after O'Donnell *et al.*[3] (red solid line). (c) FWHM of the A exciton emission versus temperature with its related standard deviation (black dots) and a fit according to eq S2 (red solid line).

Photoluminescence study at different steps of device fabrication

For a better understanding of the red-shift of the EL signal as compared to the original PL signal of the WS_2 monolayer on sapphire, a PL study of the WS_2 monolayer at different stages of the device processing is shown in Figure S2. It can be seen, that the PL signal already shifts to larger wavelength after transferring the WS_2 monolayer on top of the hole injection layer poly-TPD. After completing the device by spin-coating ZnO-QDs on top and evaporation of the Al contacts, the PL signal is further shifted to larger wavelength. The energy shift of the PL peak with substrate and environment due to a dielectric screening effect and/or charge transfer and related doping is in agreement with literature.[9,10] The shoulder in the PL spectrum of the device at around 580 nm - 600 nm can be attributed to the poly-TPD layer. Note, that in contrast to PL measurements, the supporting layers do not contribute to the EL in a fully fabricated device with WS_2 monolayer as active material.

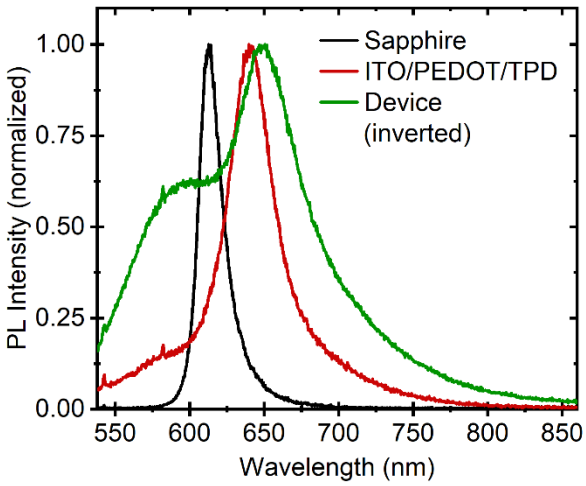

Figure S2. PL spectra of the WS_2 monolayer at different stages of the device process: As grown on sapphire (black), after transfer on top of the poly-TPD layer (red) and in the fully fabricated device (green).

Estimation of the photoluminescence quantum yield

To get access to the photoluminescence quantum yield (PLQY) of the as grown WS_2 monolayer on sapphire, first the collection efficiency of the measurement setup has to estimated.

The general equation for the detected photon number per time for any setup can be written as:

$$\frac{P_{det}}{h\nu_{det}} = \frac{P_{exc}}{h\nu_{exc}} \cdot PLQY \cdot A \cdot \beta \qquad \text{(eq S3)}$$

Here $P_{det}/h\nu_{det}$ and $P_{exc}/h\nu_{exc}$ represent the photons per time detected in the setup and exciting the sample, respectively, with P_{det} (P_{exc}) as detected (exciting) power. A is the absorbance of the sample at the excitation wavelength, $PLQY$ the photoluminescence quantum yield in the sample and β the collection efficiency of the setup.

To estimate the collection efficiency of our setup, a reflecting substrate (gold layer with reflectance of 80% at a wavelength of 532 nm) was introduced in the setup and the detected counts per second for a defined laser power were measured. In this case, $PLQY * A$ was set to $1 * 0.8 = 0.8$ and β could be determined from measuring the counts in the detector and the power of the exciting laser at the position of the sample. From this, we determined a collection efficiency $\beta = 10^{-3}$.

When characterizing the as grown WS_2 monolayers by PL, the *PLQY* could be calculated from the laser power, the detected intensity and the absorption in the monolayer that we assumed to be $A = 2\%$ at the excitation wavelength of $\lambda = 532$ nm.[11] With this procedure, we estimated the PLQY of the MOCVD WS_2 monolayer fully coalesced on sapphire to be about 10^{-2}%.

Comparison of electroluminescence under pulsed and continuous operation

Figure S3 shows a comparison of the EL spectra under a pulsed square-wave voltage and a continuous voltage, respectively. The efficiency in the pulsed EL mode is enhanced by a factor of almost 4.

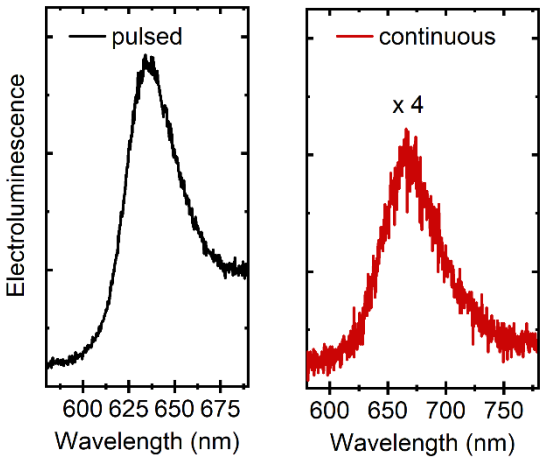

Figure S3. EL spectra recorded at 6.5 V in pulsed (left) and continuous (right) operation mode, respectively. The spectrum detected in continuous mode is multiplied by the factor of 4 to visualize the enhanced luminescence of approximately a factor of 4.

Atomic force microscopy images of the as grown WS_2 monolayer on sapphire

In order to assess the surface morphology of the WS_2 layer as grown on sapphire atomic force microscopy (AFM) has been performed (Figure S4). The root mean square (Rms) of the WS_2 covered sapphire substrate after MOVCD growth was determined to be <0.3 nm for areas without bilayer growth. This is only slightly enhanced as compared to the Rms of the sapphire substrate (0.1 nm), indicating high sample quality. The inset of Figure S4 shows a typical bilayer crystal grain on top of the coalesced WS_2 monolayer. The step height of <1 nm corresponds to the expected thickness of one additional WS_2 layer.

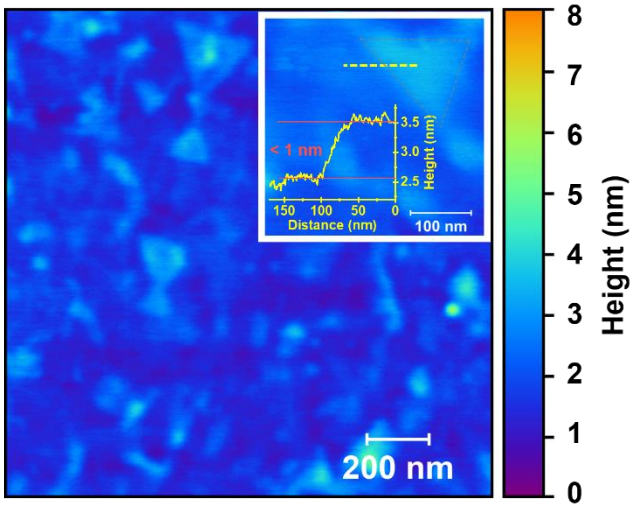

Figure S4. AFM image of WS_2 grown via MOCVD on sapphire showing the flat coalesced monolayer with a surface roughness of <0.3 nm (Rms) for the monolayer areas. In the inset a

single bilayer crystal grain on top of the coalesced monolayer is displayed. A line scan along the dashed yellow line is added demonstrating a step height <1 nm between the coalesced monolayer and the bilayer grain.

References

(1) Tongay, S.; Suh, J.; Ataca, C.; Fan, W.; Luce, A.; Kang, J. S.; Liu, J.; Ko, C.; Raghunathanan, R.; Zhou, J. *et al.* Defects activated photoluminescence in two-dimensional semiconductors: interplay between bound, charged, and free excitons. *Scientific reports* **2013**, *3*, 2657.

(2) Plechinger, G.; Nagler, P.; Kraus, J.; Paradiso, N.; Strunk, C.; Schüller, C.; Korn, T. Identification of excitons, trions and biexcitons in single-layer WS_2. *Phys. Status Solidi RRL* **2015**, *9*, 457–461.

(3) O'Donnell, K. P.; Chen, X. Temperature dependence of semiconductor band gaps. *Appl. Phys. Lett.* **1991**, *58*, 2924–2926.

(4) Wei, K.; Liu, Y.; Yang, H.; Cheng, X.; Jiang, T. Large range modification of exciton species in monolayer WS_2. *Applied optics* **2016**, *55*, 6251–6255.

(5) Rudin, S.; Reinecke, T. L.; Segall, B. Temperature-dependent exciton linewidths in semiconductors. *Phys. Rev. B* **1990**, *42*, 11218–11231.

(6) Selig, M.; Berghäuser, G.; Raja, A.; Nagler, P.; Schüller, C.; Heinz, T. F.; Korn, T.; Chernikov, A.; Malic, E.; Knorr, A. Excitonic linewidth and coherence lifetime in monolayer transition metal dichalcogenides. *Nature communications* **2016**, *7*, 13279.

(7) Molas, M. R.; Nogajewski, K.; Potemski, M.; Babiński, A. Raman scattering excitation spectroscopy of monolayer WS_2. *Scientific reports* **2017**, *7*, 5036.

(8) Yen, P. C.; Hsu, H. P.; Liu, Y. T.; Huang, Y. S.; Tiong, K. K. Temperature dependences of energies and broadening parameters of the band-edge excitons of Re-doped WS_2 and 2H-WS_2 single crystals. *J. Phys.: Condens. Matter* **2004**, *16*, 6995.

(9) Eichfeld, S. M.; Hossain, L.; Lin, Y.-C.; Piasecki, A. F.; Kupp, B.; Birdwell, A. G.; Burke, R. A.; Lu, N.; Peng, X.; Li, J. *et al.* Highly scalable, atomically thin WSe_2 grown via metal-organic chemical vapor deposition. *ACS Nano* **2015**, *9*, 2080–2087.

(10) Martín-Sánchez, J.; Mariscal, A.; Luca, M. de; Martín-Luengo, A. T.; Gramse, G.; Halilovic, A.; Serna, R.; Bonanni, A.; Zardo, I.; Trotta, R. *et al.* Effects of dielectric stoichiometry on the photoluminescence properties of encapsulated WSe_2 monolayers. *Nano Res.* **2018**, *11*, 1399–1414.

(11) Hill, H. M.; Rigosi, A. F.; Roquelet, C.; Chernikov, A.; Berkelbach, T. C.; Reichman, D. R.; Hybertsen, M. S.; Brus, L. E.; Heinz, T. F. Observation of Excitonic Rydberg States in Monolayer MoS_2 and WS_2 by Photoluminescence Excitation Spectroscopy. *Nano letters* **2015**, *15*, 2992–2997.